

Correlation and localization properties of topological charge density and the pseudoscalar glueball mass in lattice Yang-Mills theory

Abhishek Chowdhury^a, A. Harindranath^a and Jyotirmoy Maiti^b

^a*Theory Division, Saha Institute of Nuclear Physics
1/AF Bidhan Nagar, Kolkata 700064, India*

^b*Department of Physics, Barasat Government College,
10 KNC Road, Barasat, Kolkata 700124, India*

E-mail: abhishek.chowdhury@saha.ac.in, a.harindranath@saha.ac.in,
jyotirmoy.maiti@gmail.com

ABSTRACT: Using ensembles generated with periodic or open boundary conditions in the temporal direction, and using Wilson flow or HYP smearing to smoothen the gauge fields, we have studied the Topological Charge Density Correlator (TCDC) and the Inverse Participation Ratio (IPR) for the topological charge density distribution in Lattice Yang-Mills theory. We have observed that at the same lattice volume and lattice spacing and at a given Wilson flow time, there is no noticeable difference between the TCDCs calculated with periodic and open boundary conditions in the temporal direction. The size of the positive core increases and the heights of the positive and negative peaks decrease with flow time, in both the cases. Open boundary condition makes it possible to compute observables at a smaller lattice spacing. On the other hand, the reference energy scale provided by Wilson flow allows us to study their scaling behaviour. At a particular Wilson flow time t for all the lattice spacings investigated (except the largest one), the TCDC data show universal behaviour within our statistical uncertainties. The behaviour of TCDC at a fixed Wilson flow time for different lattice spacings is contrasted with that of the data at a fixed HYP smearing level which show apparent scaling violation. The pseudoscalar glueball mass extracted from the TCDC appears to be insensitive to the lattice spacings ($0.0345 \text{ fm} \leq a \leq 0.0667 \text{ fm}$) explored in this work. Expectation values of the IPR at different lattice spacings are found to be very close to each other at a given reference scale.

Contents

1	Motivation	1
2	Methodology	2
3	Simulation Parameters	3
4	Numerical Results	4
4.1	Topological charge density correlator	4
4.2	Extraction of pseudoscalar glueball mass from TCDC	7
4.3	Localization properties of topological charge density	10
5	Conclusions	14

1 Motivation

The negativity of the Topological Charge Density Correlator (TCDC) for non-zero distances as a consequence of the reflection positivity and the pseudoscalar nature of the relevant local operator in Euclidean field theory is well-known [1, 2]. The non-trivial implication of the negativity of TCDC for the structure of topological charge density in QCD vacuum has been investigated in detail [3]. Various aspects of TCDC in quenched and full QCD have been carried out in Ref. [4] and [5]. A thorough investigation of the mechanisms leading to the suppression of the topological susceptibility with decreasing quark mass, based on the properties of TCDC has been carried out [6] in two-flavour QCD.

There remain several open issues related to the topological charge density $q(x)$ and TCDC in non-abelian gauge theories. An important issue is the scaling of TCDC as one approaches the continuum limit. It is however well-known that current lattice gauge theory simulations employing periodic boundary condition in the temporal direction are handicapped by the trapping of topological charge in a particular sector, as the lattice spacing is reduced so as to reach the continuum limit. Open boundary condition in the temporal direction has been proposed and investigated [7–9] as a (partial) cure to this problem. Also see, ref. [10]. Open boundary condition, however, introduces undesirable boundary effects. One needs to have quantitative estimates of the boundary artifacts by comparing results for TCDC with both open and periodic boundary conditions in the temporal directions. One can then probe TCDC for even smaller lattice spacings and address questions related to the scaling etc.

The famous Witten-Veneziano formula [11, 12] relates η' mass to the topological susceptibility in pure Yang-Mills theory. For the calculation of $q(x)$, ref. [13] uses the algebraic definition of the field strength tensor. To overcome the potential lattice artifacts associated with the algebraic definition of the topological charge density $q(x)$ on the lattice and

severe singularities present in TCDC in the continuum theory, various proposals have been studied in the literature. In ref. [14], $q(x)$ based on Ginzparg-Wilson fermion has been employed, whereas refs. [15, 16] utilize a proposal designed to overcome short distance singularities. A spectral projection formula designed to be free from singularity is employed in ref. [17] which compares the result for topological susceptibility χ using algebraic definition. Since ref. [17] has established that the results for χ using various approaches are in agreement with each other within statistical uncertainties, in this work we employ the algebraic definition for $q(x)$.

Among the available algebraic definitions for $q(x)$, one is based on the clover expression for the field strength $F_{\mu\nu}$ which is the simplest. Another is the more sophisticated ten-link definition developed for $SU(2)$ by DeGrand, Hasenfratz and Kovacs [18], modified for $SU(3)$ by Hasenfratz and Neiter [19]. For our calculations, the clover definition has been employed unless otherwise stated. With the adoption of the algebraic definition, to suppress unwanted lattice artifacts, smearing of gauge fields is necessary. In our past study of TCDC [6], we have employed HYP smearing [20]. However, the recently proposed Wilson flow [21–23] makes smearing a well-defined mathematical procedure and in addition, provides a common reference scale to extract physical quantities from lattice calculations employing different lattice spacings. Such a reference scale, which for example has been used in pure Yang-Mills theory to compare topological susceptibility calculated at different lattice scales [24], is essential when we address the issue of scaling of TCDC, etc. Similar calculations have been performed recently also for dynamical fermions [25].

It is also useful to compare HYP smearing with Wilson flow in the case of TCDC, as we have done for the extraction of scalar glueball mass [26]. It will be also very interesting to extract the pseudoscalar glueball mass from the tail region of the TCDC and study its scaling properties at a given Wilson flow time.

In addition to the properties of the correlator of topological charge density, its localization property itself is also of interest. There exists a body of literature on the localization properties of the low-lying Dirac eigen modes [27], because of their connection with the topological properties of the QCD vacuum. However, the localization properties of the topological charge density based on the algebraic definition involving the field strength $F_{\mu\nu}$ seems to have attracted little attention except for a preliminary study by the MILC collaboration [28]. It is interesting to study the Inverse Participation Ratio (IPR) associated with the topological charge density distribution and compare their behaviour under Wilson flow and HYP smearing. A direct visualization of the effect of Wilson flow on topological charge density distribution of typical gauge configurations will also shed light on their localization properties.

2 Methodology

We summarize here the working formulae for the observables computed in this study and the expressions used to analyze the data. The topological charge density correlator is given by

$$C(r) = \langle q(x)q(y) \rangle, \quad r = |x - y| \quad (2.1)$$

where $q(x)$ is the topological charge density. In order to analyze the lattice data, the functional form of the correlator in the negative r region is approximated by the negative of free scalar propagator (see refs. [32] and [33])

$$\langle \phi(x)\phi(y) \rangle = \frac{m}{4\pi^2 r} K_1(mr) \quad (2.2)$$

where $K_1(z)$ is a modified Bessel function whose asymptotic form is given by

$$K_1(z) \underset{\text{large } z}{\sim} e^{-z} \sqrt{\frac{\pi}{2z}} \left[1 + \frac{3}{8z} \right]. \quad (2.3)$$

The asymptotic formula given above is appropriate for unsmeared fields whereas in practice smeared fields are used to compute the correlator. Unlike other smearing techniques, Wilson flow allows one to calculate the correlator in an analytical form. With Wilson flow, the smeared correlator

$$C_t(r) = \langle \phi_t(x)\phi_t(y) \rangle \quad (2.4)$$

where

$$\phi_t(x) = \int d^4 z \frac{e^{-\frac{(x-z)^2}{4t}}}{(4\pi t)^2} \phi(z) e^{-m^2 t}, \quad (2.5)$$

takes the form

$$C_t(r) = e^{-2m^2 t} \frac{m}{16\pi^2} \int d^4 s \frac{e^{-\frac{(r-s)^2}{8t}}}{(4\pi t)^2} \frac{1}{|s|} K_1(m|s|) \quad (2.6)$$

$$= e^{-2m^2 t} e^{-\frac{r^2}{8t}} \frac{m}{4\pi^2 r t} \int_0^\infty ds s e^{-\frac{s^2}{8t}} I_1(rs/(4t)) K_1(ms) \quad (2.7)$$

where I_1 is a modified Bessel function.

To investigate the localization property of the topological charge density $q(x)$, one uses the IPR defined as

$$\text{IPR} = V \frac{\sum_x |q(x)|^4}{(\sum_x |q(x)|^2)^2} \quad (2.8)$$

where V is the four dimensional lattice volume.

3 Simulation Parameters

In table 1, we present simulation parameters for the HMC algorithm used to generate configurations with open and periodic boundary condition in the temporal direction with unimproved Wilson gauge action. We also give the number of configurations used for measurements of TCDC and IPR. The gaps between two successive measurements have been chosen such that the measurements are statistically independent of each other.

With periodic boundary condition, in order to increase statistics source averaging is usually performed for the measurement of TCDC. However, with open boundary condition, translational invariance in the temporal direction is absent. In order to avoid boundary effects, to calculate TCDC, the source is kept at the mid-point of the temporal extent

Lattice	Volume	β	N_{cnfg}	Gap	N_0	τ	$a[\text{fm}]$	t_0/a^2
O_1	$24^3 \times 48$	6.21	401	392	12	3	0.0667(5)	6.207(15)
O_2	$32^3 \times 64$	6.42	405	240	20	4	0.0500(4)	11.228(31)
O_3	$48^3 \times 96$	6.59	404	160	26	5	0.0402(3)	17.630(53)
O_4	$64^3 \times 128$	6.71	74	160	64	10	0.0345(4)	24.279(227)
P_1	$24^3 \times 48$	6.21	401	280	12	3	0.0667(5)	6.197(15)
P_2	$32^3 \times 64$	6.42	401	176	20	4	0.0500(4)	11.270(38)
P_3	$48^3 \times 96$	6.59	191	64	26	5	0.0402(3)	18.048(152)

Table 1. Simulation parameters for the HMC algorithm. N_0 is the number of integration steps, τ is the trajectory length and t_0/a^2 is the dimensionless reference Wilson flow time. O and P refer to ensembles with open and periodic boundary condition in the temporal direction.

and we perform average over the spatial volume of the lattice. Since we want to compare the results with open and periodic boundary conditions, we adapt same source averaging procedure for latter case also. To determine lattice spacings (see table 1), we have used results from Refs. [29, 30].

4 Numerical Results

4.1 Topological charge density correlator

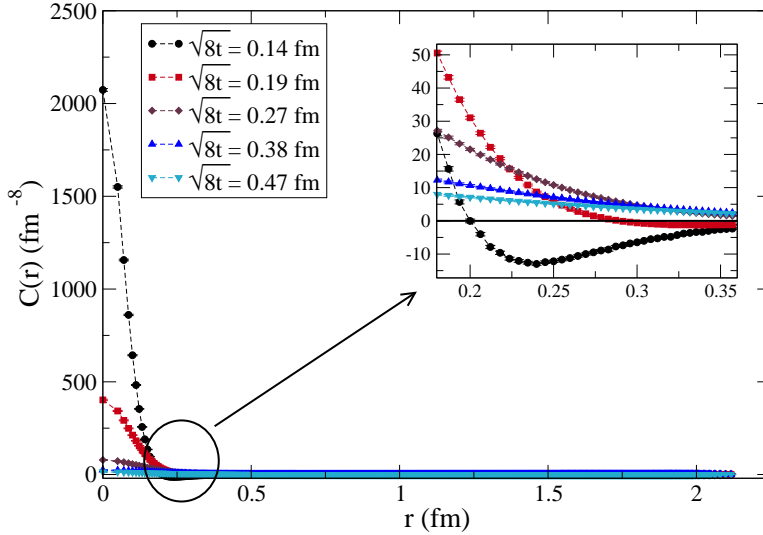


Figure 1. Plot of topological charge density correlator $C(r)$ versus r at various value of Wilson flow time $\sqrt{8t}$ at $\beta = 6.42$ and lattice volume $32^3 \times 64$ for ensemble P_2 .

In figure 1, we plot the behaviour of $C(r)$ versus r at various Wilson flow times $\sqrt{8t}$ at $\beta = 6.42$ and lattice volume $32^3 \times 64$ for ensemble P_2 . Topological charge density which is constructed from the clover definition of the field strength tensor further gets extended with Wilson flow time. As expected, in figure 1, the size of the positive core increases with Wilson flow time. Note that, further, the heights of the positive and negative peaks decrease with flow time. Since with flow the effective size of the charge density increases, two charge densities eventually overlap completely resulting in the disappearance of the negative region of $C(r)$.

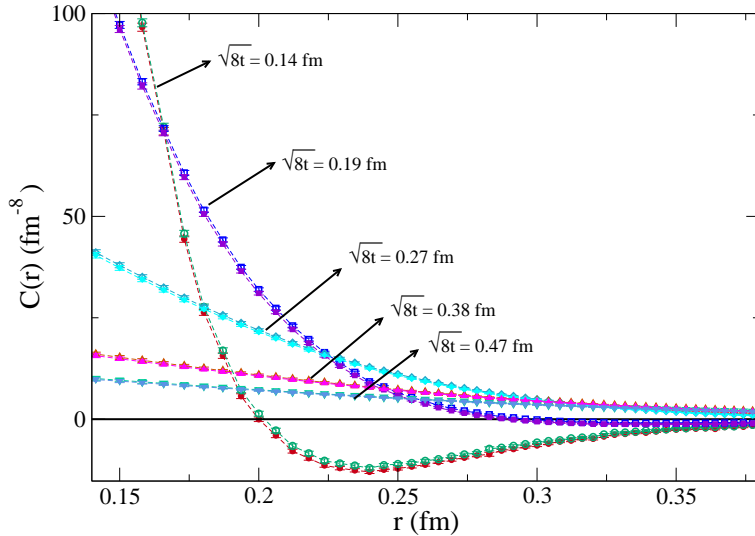


Figure 2. Comparison of $C(r)$ versus r at various value of Wilson flow time $\sqrt{8t}$ at $\beta = 6.42$ and lattice volume $32^3 \times 64$ for ensembles P_2 (filled symbols) and O_2 (open symbols).

In figure 2, we compare TCDC for the ensembles P_2 and O_2 . As already stated the source is placed at the mid-point of the temporal extent and the sink is placed all over the lattice. We note that there is no noticeable difference between the two TCDC at a given Wilson flow time.

Unlike conventional smearing techniques, Wilson flow provides an energy scale ($\frac{1}{\sqrt{8t}}$) at which observables can be probed. In order to check possible scaling violation in TCDC, one has to choose a particular Wilson flow time for all the lattice spacings investigated. In figure 3, we plot TCDC for ensembles O_1 , O_2 , O_3 and O_4 at the Wilson flow time $\sqrt{8t} = 0.14$ fm (the rationale for choosing the scale to be 0.14 fm will be explained later). Except the data corresponding to the largest lattice spacing, the data show universal behaviour within our statistical uncertainties.

In conventional smearing techniques like HYP smearing, a fixed smearing level does not correspond to a common energy scale to compare data generated at different lattice spacings. Whereas in case of Wilson flow, it corresponds to a fixed value of t/a^2 for all a and

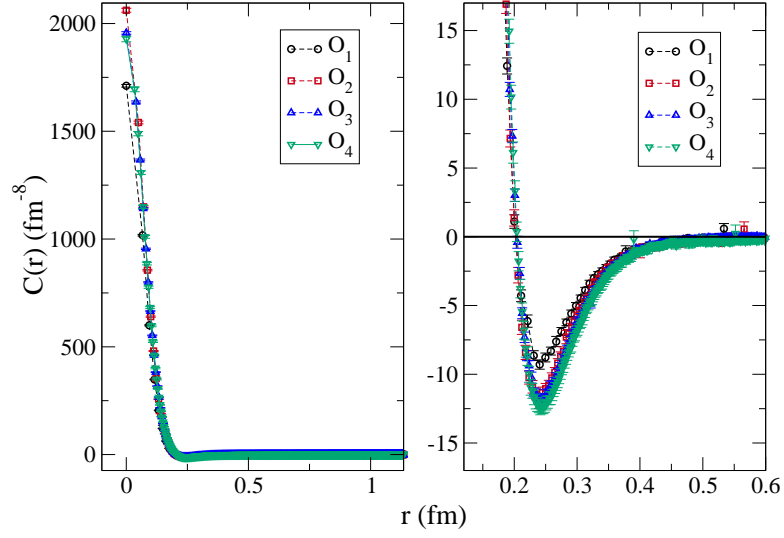


Figure 3. $C(r)$ versus r at Wilson flow time $\sqrt{8t} = 0.14$ fm for ensembles O_1 , O_2 , O_3 and O_4 .

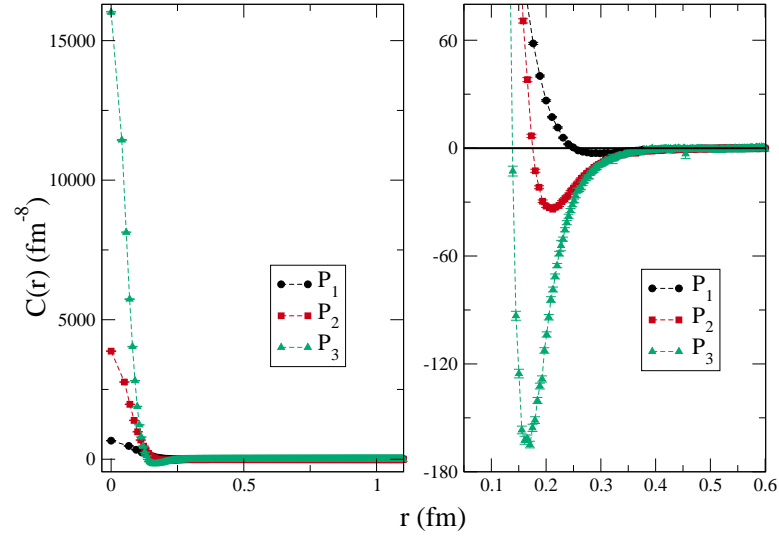


Figure 4. $C(r)$ versus r at 3 HYP smearing steps for ensembles P_1 , P_2 and P_3 .

hence corresponds to different energy scales at different lattice spacings. This is illustrated in the figure 4 where TCDCs at various lattice scales are compared at the same smearing

level 3 (HYP). From the exhibited behaviour one may infer large scaling violations but one should keep in mind that a fixed HYP smearing level at different lattice spacings does not correspond to a common energy scale. This is to be contrasted with Wilson flow case, which facilitates the use of a common energy scale, shown in the figure 3.

Recently a comparison of Wilson flow with cooling has been performed [34] where a relation between Wilson flow time and the number of cooling steps has been established. We have investigated whether one can phenomenologically establish a relation between Wilson flow time and HYP smearing level. In the case of TCDC, we found that it is not possible to establish such a relation even at a fixed lattice spacing, valid for all r . Some approximate relation, of course can be found, which however, will vary with lattice spacing.

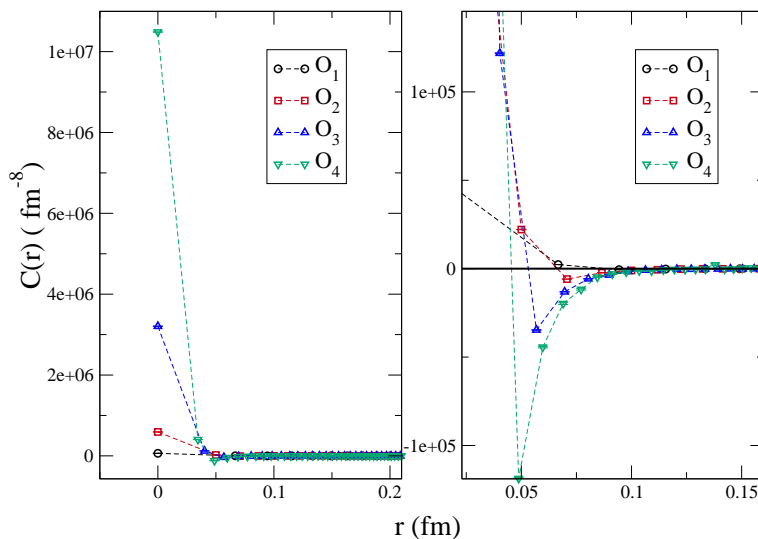


Figure 5. Plot of $C(r)$ versus r for ensembles O_1 , O_2 , O_3 and O_4 without smoothing of gauge fields.

In the figure 5, we plot the unsmoothed TCDC for the ensembles O_1 , O_2 , O_3 and O_4 . In this case, presence of severe lattice artifacts prevents one from extracting any physical observable. For example one can not extract the topological susceptibility from such data. Nevertheless we find that the correlator exhibits the negativity as expected for the correlator of pseudo scalar operator. Further we find that the radius of the positive core shrinks with lattice spacing as per expectation.

4.2 Extraction of pseudoscalar glueball mass from TCDC

Encouraged by the universal behaviour exhibited by the TCDC for different lattice spacings at a common Wilson flow time, we proceed to extract the lowest pseudoscalar glueball mass from the tail region of the TCDC. In the past MILC collaboration [33] checked the consistency of their quenched correlator data with pseudoscalar glueball mass extracted in

Ref. [31], without actually fitting the data. In this case, a particular level of HYP smearing is used to smooth the gauge configurations at different lattice spacings. As shown in previous section, in conventional smearing techniques like HYP smearing, a fixed smearing level does not correspond to a common energy scale to compare data generated at different lattice spacings. However, the method of Wilson flow allows to compute observables at a given energy scale.

Due to large vacuum fluctuations present in the correlators of gluonic observables, the extraction of glueball masses is much more difficult compared to hadron masses. Further, the pseudoscalar glueball mass is expected to be much higher than scalar glueball mass. Thus one needs larger statistics and lower lattice spacings for the extraction of pseudoscalar glueball mass. Apart from the cost associated with generating configurations, the cost of measuring all to all radial correlator also increases rapidly as one goes to smaller lattice spacings keeping the physical volume constant. Among our ensembles, O_2 and P_2 are the best from the considerations of statistics as well as lattice spacings.

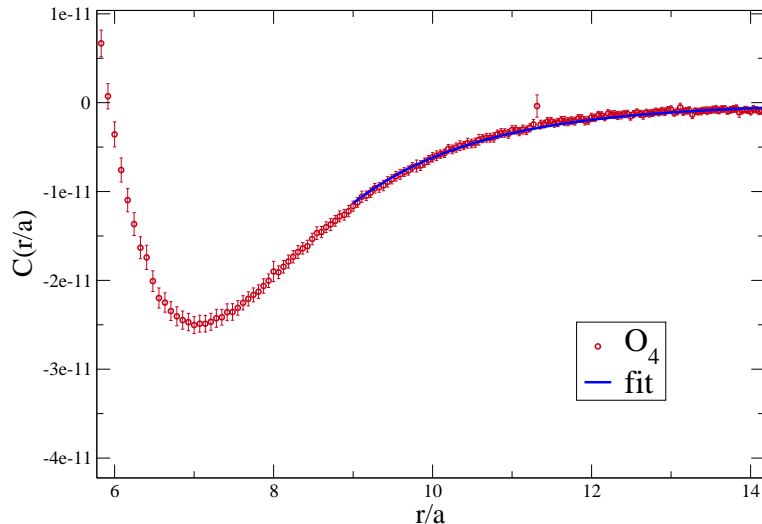


Figure 6. $C(r/a)$ versus r/a for the ensemble O_4 at Wilson flow time $\sqrt{8t} = 0.14$ fm. Also shown is the the fit used to extract the pseudoscalar glueball mass.

In figure 6, the TCDC $C(r/a)$ is plotted versus r/a for the ensemble O_4 at Wilson flow time $\sqrt{8t} = 0.14$ fm. Also shown is the fit in large r region with formula 2.3 to extract the pseudoscalar glueball mass. In the fitting procedure the amplitude and the mass are treated as free parameters. We studied the stability of the fit results (mass and amplitude) with fitting range by varying both the initial and the final values of r/a in the tail region of TCDC. The extracted mass values for different ensembles are given in table 2.

In order to extract the pseudoscalar glueball mass in the continuum, in figure 7 we plot the mass in MeV versus a^2 in fm^2 for both the boundary conditions for all the lattice

Lattice	am	m (MeV)
O_1	0.887(39)	2624(114)
P_1	0.831(36)	2459(108)
O_2	0.648(18)	2559(73)
P_2	0.647(19)	2554(75)
O_3	0.605(17)	2972(82)
P_3	0.511(11)	2506(55)
O_4	0.427(9)	2444(51)

Table 2. Pseudoscalar glueball mass.

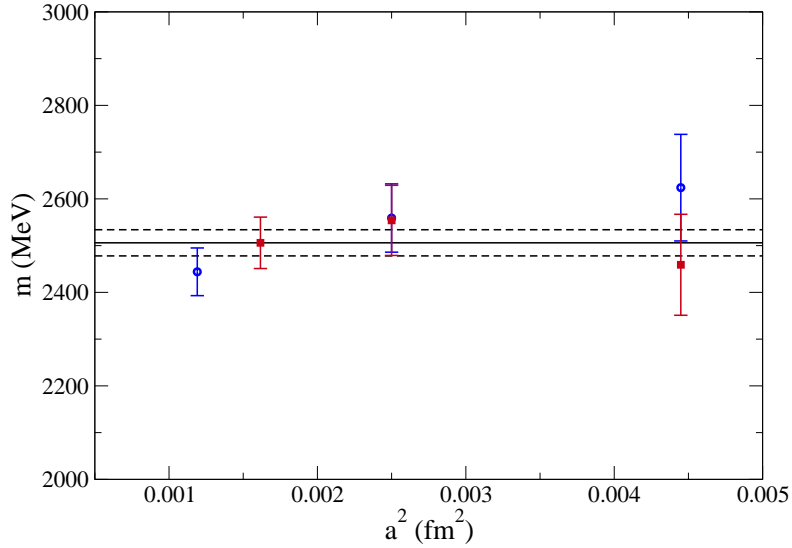


Figure 7. Plot of lowest pseudoscalar glueball mass versus a^2 for both open and periodic boundary conditions at Wilson flow time $\sqrt{8t} = 0.14$ fm. Also shown is the fit to the data.

spacings explored in this work. In the figure, we have dropped the data point corresponding to the ensemble O_3 which appears to be affected by some unaccounted systematic errors. As expected from the universal scaling behaviour exhibited by $C(r)$ in the asymptotic region (see figure 3) within the statistical error, the data for mass does not show any deviation from scaling. Hence we fit a constant to the data as shown in the figure and thus extract the continuum value of the pseudoscalar glueball mass with the result as 2506 (28) MeV. This value compares very well with the value 2560 (35) MeV quoted in ref. [31], which is extracted from the decay of the temporal pseudoscalar correlator on an anisotropic lattice.

Since TCDC has severe singularities and lattice artifacts, smoothing of gauge fields is mandatory. Undersmearing of gauge fields leads to persisting lattice artifacts while

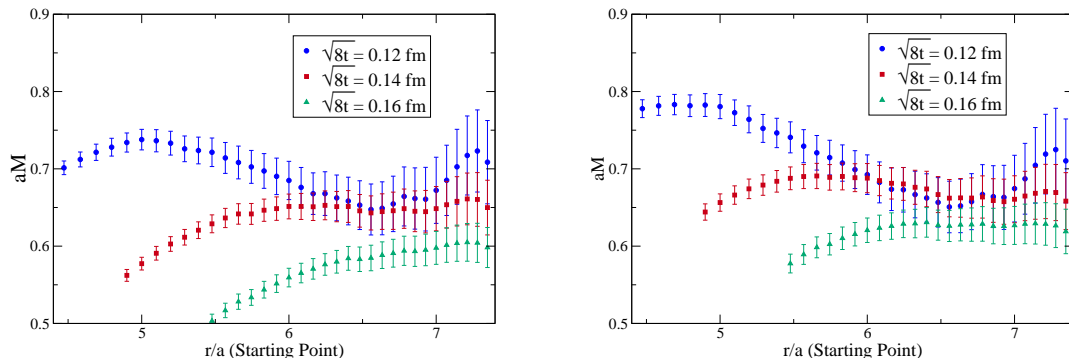


Figure 8. Sensitivity, to starting point of fit range for fixed end point, of pseudoscalar glueball mass extracted using asymptotic formula (left) and smearing formula (right) for ensemble P_2 with three Wilson flow times.

oversmearing may wipe out even the negativity character of the correlator. Thus there is an optimal range of smearing for which one can reliably extract useful information from the lattice data. We have studied the behaviour of the extracted pseudoscalar glueball mass under different Wilson flow times. In figure 8 (left), we show the sensitivity, to starting point of fit range for a fixed end point, of pseudoscalar glueball mass extracted using asymptotic formula in eqn. (2.3). The extracted mass is apparently stable at and around the scale 0.14 fm as exhibited in the overlap of plateau regions of data for three different Wilson flow times. Corresponding behaviour for the fit results obtained using smearing formula in eqn. (2.7) is shown in figure 8 (right). Latter clearly confirms the stability around the scale 0.14 fm. This guided us to take 0.14 fm as the common scale to study various observables for different ensembles. However at this scale, the fit results for pseudoscalar glueball mass obtained using the smearing formula do not show any significant difference with that obtained using the asymptotic formula. That is why we have used the asymptotic formula to extract the mass for all other ensembles as well.

4.3 Localization properties of topological charge density

To investigate the effect of Wilson flow on the localization property of topological charge density, we plot the configuration average of IPR versus Wilson flow time (t/a^2) in figure 9 for the ensembles P_1 , P_2 and P_3 . We note that $\langle IPR \rangle$ monotonously increases with t/a^2 indicating increasing localization of $q(x)$. Also, *throughout* the range of t/a^2 , $\langle IPR \rangle$ appears to decrease with decreasing lattice spacing.

Since Wilson flow provides a scale (independent of the lattice spacing) to probe the observables, it is more interesting to study the variation of $\langle IPR \rangle$ with respect to t/r_0^2 with r_0 being the Sommer parameter, for ensembles at different lattice spacings¹. In figure 10 we plot $\langle IPR \rangle$ versus t/r_0^2 for ensembles P_1 , P_2 and P_3 . We find that, remarkably, unlike the behaviour shown in figure 9, the average IPR's for different ensembles are now very

¹There is nothing special about t/r_0^2 , one can plot it in physical unit ($\sqrt{8t}$) also.

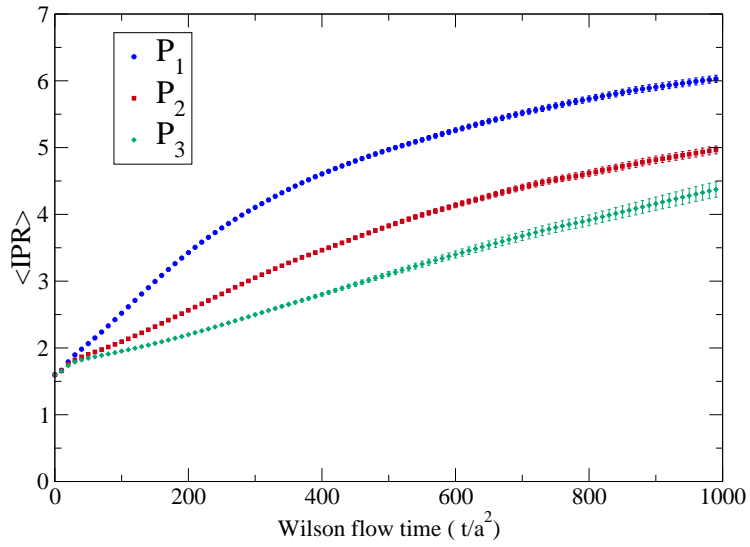


Figure 9. Plot of configuration average of Inverse Participation Ratio ($\langle IPR \rangle$) versus Wilson flow time (t/a^2) for the ensembles P_1 , P_2 and P_3 .

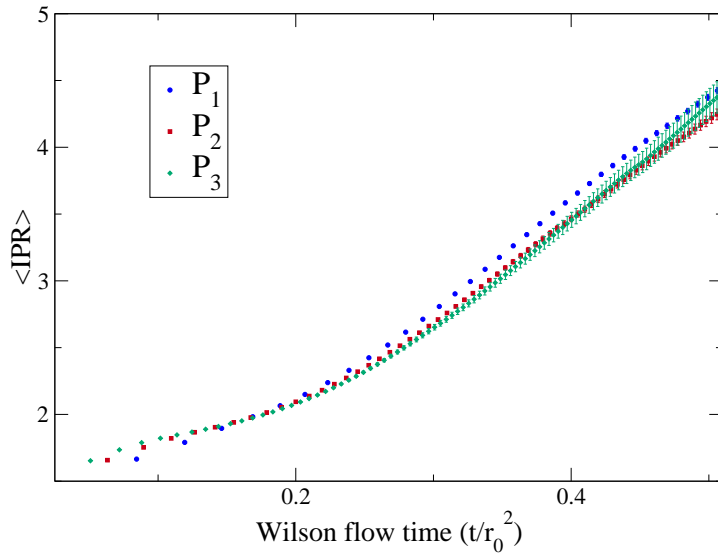


Figure 10. $\langle IPR \rangle$ versus t/r_0^2 for ensembles P_1 , P_2 and P_3 .

close to each other and the average IPR's for the ensembles corresponding to the smaller two lattice spacings agree with each other within our statistical accuracy. The data for ensembles corresponding to the largest lattice spacing ($\beta = 6.21$) exhibits some mild scaling violation as already noted in the case of TCDC in figure 3.

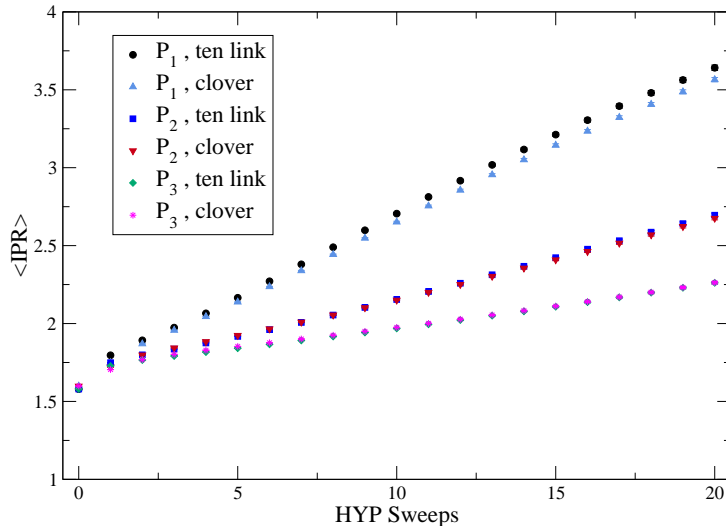


Figure 11. Plot of $\langle \text{IPR} \rangle$ versus HYP sweeps using two definitions of the topological charge density (clover and ten link) for ensembles P_1 , P_2 and P_3 .

In figure 11, we plot $\langle \text{IPR} \rangle$ versus HYP sweeps using two definition of topological charge density (clover and ten link) for ensembles P_1 , P_2 and P_3 . It is expected that different lattice discretizations of the topological charge density yield the same physical observable as one approaches the continuum limit. We note that the $\langle \text{IPR} \rangle$ for the two definitions of topological charge density move closer to each other with decreasing lattice spacing, as expected.

We also note that $\langle \text{IPR} \rangle$ decreases with decreasing lattice spacing at a given flow time. The behaviour we have observed appears compatible with that exhibited by the data of MILC collaboration [28] at their three smaller lattice spacings. Note that the largest lattice spacing explored in our work is smaller than the smallest lattice spacing studied in Ref. [28] which, however, has employed an improved lattice action.

In order to gain a better understanding of the behaviour of both the charge density correlator $C(r)$ and the inverse participation ratio (IPR) we plot, in figure 12, the behaviour of the topological charge density distribution $q(x)$ under Wilson flow, as a function of x_0 and x_1 at $x_2 = x_3 = 24$ for a typical configuration belonging to the ensemble O_3 . The plots (a) to (f) correspond to the flow times $\sqrt{8t} = 0.14, 0.19, 0.25, 0.3, 0.38$ and 0.47 fm respectively. At relatively small values of the Wilson flow time, it is seen that $q(x)$ possesses regions of both positive and negative charge densities of relatively large magnitudes lying

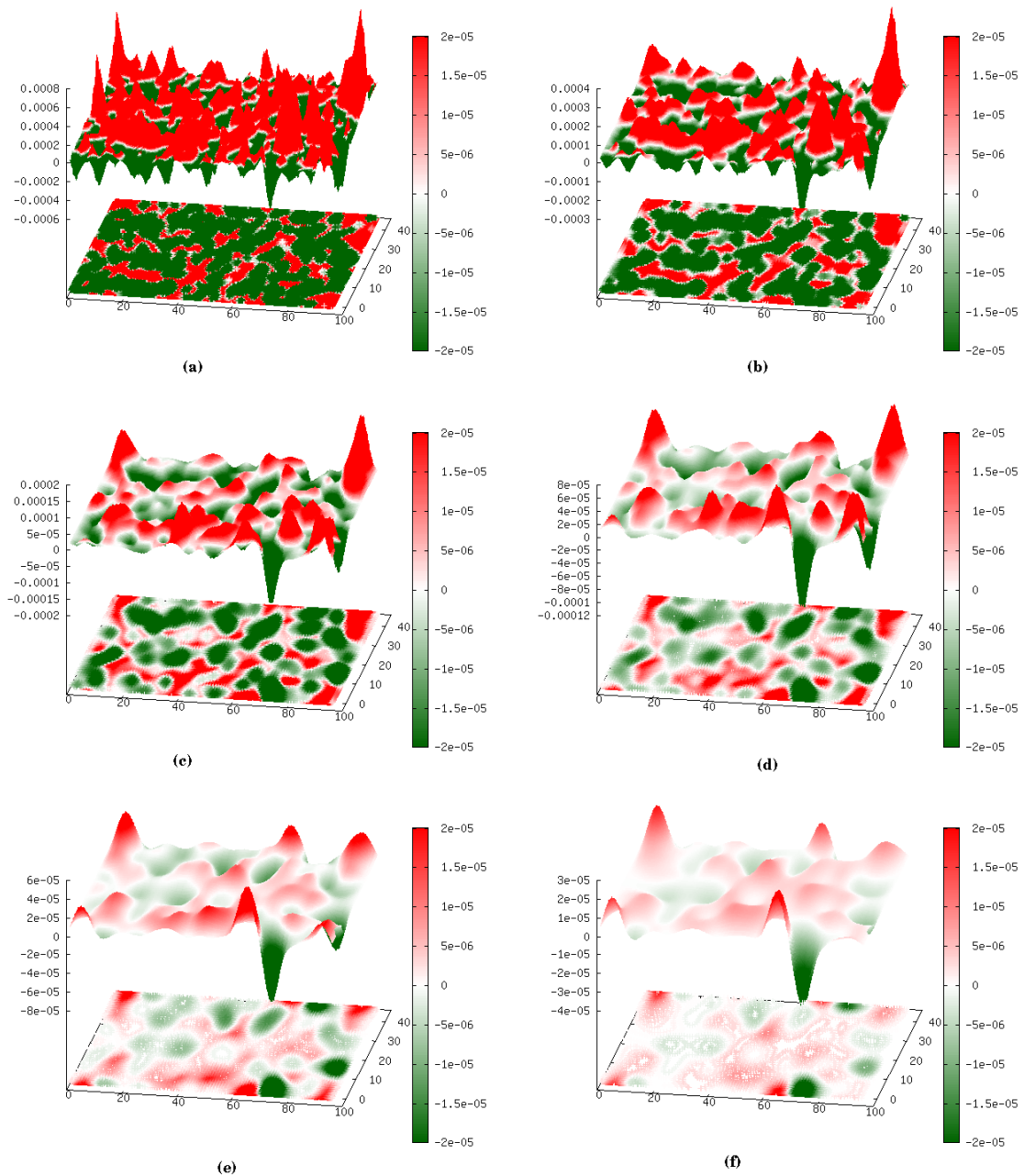


Figure 12. The behaviour of the topological charge density distribution $q(x)$ under Wilson flow, as a function of x_0 and x_1 at $x_2 = x_3 = 24$ for a typical configuration belonging to the ensemble O_3 . The plots (a) to (f) correspond to the flow times $\sqrt{8t} = 0.14, 0.19, 0.25, 0.3, 0.38$ and 0.47 fm respectively.

next to each other. This provides a qualitative explanation[35] of the positive core and the adjoining negative peak observed in $C(r)$. As the Wilson flow time increases, the proximity of the regions of positive and negative charge densities of large magnitudes diminishes, and the charge density appears to be more localized. This results in reduced participation for $q(x)$ which in turn, explains the increase of IPR with Wilson flow time.

5 Conclusions

We have observed that at a given Wilson flow time, there is no observable difference between the TCDCs calculated with periodic and open boundary conditions in the temporal direction at the same lattice volume and lattice spacing. In both the cases, the size of the positive core increases and the heights of the positive and negative peaks decrease with flow time. With open boundary condition, we are able to measure TCDC at a smaller lattice spacing. Choosing a particular Wilson flow time t for all the lattice spacings investigated, we find that, except the data corresponding to the largest lattice spacing, the TCDC data show universal behaviour within our statistical uncertainties. This is in contrast to the behaviour of the data for different lattice spacings at a fixed HYP smearing level. The pseudoscalar glueball mass obtained from the tail region of TCDC does not exhibit any noticeable scaling violation and the extracted value in the continuum, 2506 (28) MeV agrees well with the value extracted previously in the literature with anisotropic lattices. We found that the configuration average of the inverse participation ratio for topological charge density, when calculated at a given level of smearing (for Wilson flow, it is t/a^2), decreases with the lattice spacing. However when plotted versus common scale t/r_0^2 , it seems to be independent of lattice spacing.

Acknowledgements

To carry out all the numerical calculations reported in this work, Cray XT5 and Cray XE6 systems supported by the 11th-12th Five Year Plan Projects of the Theory Division, SINP under the Department of Atomic Energy, Govt. of India, are used. For the prompt maintenance of the systems and the help in data management, we thank Richard Chang. We thank Pushan Majumdar and Santanu Mondal for useful discussions. This work was in part based on the publicly available lattice gauge theory code `openQCD` [36] and that of MILC collaboration [37].

References

- [1] E. Seiler and I. O. Stamatescu, *Some remarks on the Witten-Veneziano formula for the Eta-prime mass*, MPI-PAE/PTh 10/87, unpublished.
- [2] E. Seiler, *Some more remarks on the Witten-Veneziano formula for the eta-prime mass*, Phys. Lett. B **525**, 355 (2002) [hep-th/0111125].
- [3] I. Horvath, S. J. Dong, T. Draper, F. X. Lee, K. F. Liu, N. Mathur, H. B. Thacker and J. B. Zhang, *Low dimensional long range topological charge structure in the QCD vacuum*, Phys. Rev. D **68**, 114505 (2003) [hep-lat/0302009].
- [4] I. Horvath, A. Alexandru, J. B. Zhang, Y. Chen, S. J. Dong, T. Draper, K. F. Liu, N. Mathur, S. Tamhankar and H. B. Thacker, *The Negativity of the overlap-based topological charge density correlator in pure-gluon QCD and the non-integrable nature of its contact part*, Phys. Lett. B **617**, 49 (2005) [hep-lat/0504005].

- [5] F. Bruckmann, F. Gruber, N. Cundy, A. Schafer and T. Lippert, *Topology of dynamical lattice configurations including results from dynamical overlap fermions*, Phys. Lett. B **707**, 278 (2012) [arXiv:1107.0897 [hep-lat]].
- [6] A. Chowdhury, A. K. De, A. Harindranath, J. Maiti and S. Mondal, *Topological charge density correlator in Lattice QCD with two flavours of unimproved Wilson fermions*, JHEP **1211**, 029 (2012) [arXiv:1208.4235 [hep-lat]].
- [7] M. Lüscher, *Topology, the Wilson flow and the HMC algorithm*, PoS LATTICE **2010**, 015 (2010) [arXiv:1009.5877 [hep-lat]].
- [8] M. Lüscher and S. Schaefer, *Lattice QCD without topology barriers*, JHEP **1107**, 036 (2011) [arXiv:1105.4749 [hep-lat]].
- [9] M. Lüscher and S. Schaefer, *Lattice QCD with open boundary conditions and twisted-mass reweighting*, Comput. Phys. Commun. **184**, 519 (2013) [arXiv:1206.2809 [hep-lat]].
- [10] M. Grady, *Connecting phase transitions between the 3-d $O(4)$ Heisenberg model and 4-d $SU(2)$ lattice gauge theory*, arXiv:1104.3331 [hep-lat].
- [11] E. Witten, *Current Algebra Theorems for the $U(1)$ Goldstone Boson*, Nucl. Phys. B **156**, 269 (1979).
- [12] G. Veneziano, *$U(1)$ Without Instantons*, Nucl. Phys. B **159**, 213 (1979).
- [13] S. Dürr, Z. Fodor, C. Hoelbling and T. Kurth, *Precision study of the $SU(3)$ topological susceptibility in the continuum*, JHEP **0704**, 055 (2007) [hep-lat/0612021].
- [14] L. Del Debbio, L. Giusti and C. Pica, *Topological susceptibility in the $SU(3)$ gauge theory*, Phys. Rev. Lett. **94**, 032003 (2005) [hep-th/0407052].
- [15] M. Luscher, *Topological effects in QCD and the problem of short distance singularities*, Phys. Lett. B **593**, 296 (2004) [hep-th/0404034].
- [16] L. Giusti and M. Luscher, *Chiral symmetry breaking and the Banks-Casher relation in lattice QCD with Wilson quarks*, JHEP **0903**, 013 (2009) [arXiv:0812.3638 [hep-lat]].
- [17] M. Lüscher and F. Palombi, *Universality of the topological susceptibility in the $SU(3)$ gauge theory*, JHEP **1009**, 110 (2010) [arXiv:1008.0732 [hep-lat]].
- [18] T. A. DeGrand, A. Hasenfratz, T. G. Kovacs, *Topological structure in the $SU(2)$ vacuum*, Nucl. Phys. **B505**, 417-441 (1997). [arXiv:hep-lat/9705009 [hep-lat]].
- [19] A. Hasenfratz, C. Nieter, *Instanton content of the $SU(3)$ vacuum*, Phys. Lett. **B439**, 366-372 (1998). [hep-lat/9806026].
- [20] A. Hasenfratz and F. Knechtli, *Flavor symmetry and the static potential with hypercubic blocking*, Phys. Rev. D **64**, 034504 (2001) [hep-lat/0103029].
- [21] M. Lüscher, *Trivializing maps, the Wilson flow and the HMC algorithm*, Commun. Math. Phys. **293**, 899 (2010) [arXiv:0907.5491 [hep-lat]].
- [22] M. Lüscher, *Properties and uses of the Wilson flow in lattice QCD*, JHEP **1008**, 071 (2010) [arXiv:1006.4518 [hep-lat]].
- [23] M. Lüscher and P. Weisz, *Perturbative analysis of the gradient flow in non-abelian gauge theories*, JHEP **1102**, 051 (2011) [arXiv:1101.0963 [hep-th]].
- [24] A. Chowdhury, A. Harindranath, J. Maiti and P. Majumdar, *Topological susceptibility in lattice Yang-Mills theory with open boundary condition*,

- [arXiv:1311.6599 [hep-lat]].
- [25] M. Bruno, S. Schaefer and R. Sommer, *Topological susceptibility and the sampling of field space in $N_f = 2$ lattice QCD simulations*, arXiv:1406.5363 [hep-lat].
 - [26] A. Chowdhury, A. Harindranath and J. Maiti, *Open Boundary Condition, Wilson Flow and the Scalar Glueball Mass*, JHEP **1406**, 067 (2014) [arXiv:1402.7138 [hep-lat]].
 - [27] For a review, see, P. de Forcrand, *Localization properties of fermions and bosons*, AIP Conf. Proc. **892**, 29 (2007) [hep-lat/0611034].
 - [28] C. Aubin *et al.* [MILC Collaboration], *The Scaling dimension of low lying Dirac eigenmodes and of the topological charge density*, Nucl. Phys. Proc. Suppl. **140**, 626 (2005) [hep-lat/0410024].
 - [29] M. Guagnelli *et al.* [ALPHA Collaboration], *Precision computation of a low-energy reference scale in quenched lattice QCD*, Nucl. Phys. B **535**, 389 (1998) [hep-lat/9806005].
 - [30] S. Necco and R. Sommer, *The $N_f = 0$ heavy quark potential from short to intermediate distances*, Nucl. Phys. B **622**, 328 (2002) [hep-lat/0108008].
 - [31] Y. Chen, A. Alexandru, S. J. Dong, T. Draper, I. Horvath, F. X. Lee, K. F. Liu and N. Mathur *et al.*, *Glueball spectrum and matrix elements on anisotropic lattices*, Phys. Rev. D **73**, 014516 (2006) [hep-lat/0510074].
 - [32] E. V. Shuryak and J. J. M. Verbaarschot, *Screening of the topological charge in a correlated instanton vacuum*, Phys. Rev. D **52**, 295 (1995) [hep-lat/9409020].
 - [33] A. Bazavov *et al.* [MILC Collaboration], *Topological susceptibility with the asqtad action*, Phys. Rev. D **81**, 114501 (2010) [arXiv:1003.5695 [hep-lat]].
 - [34] C. Bonati and M. D’Elia, *Comparison of the gradient flow with cooling in $SU(3)$ pure gauge theory*, Phys. Rev. D **89**, 105005 (2014) [arXiv:1401.2441 [hep-lat]].
 - [35] S. Ahmad, J. T. Lenaghan and H. B. Thacker, *Coherent topological charge structure in $CP^{(N-1)}$ models and QCD*, Phys. Rev. D **72**, 114511 (2005) [hep-lat/0509066].
 - [36] <http://luscher.web.cern.ch/luscher/openQCD/>
 - [37] <http://physics.indiana.edu/sg/milc.html>.